Annual Review of Fluid Mechanics

The Fluid Mechanics of Tidal Stream Energy Conversion

Thomas A.A. Adcock,[1] Scott Draper,[2] Richard H.J. Willden,[1] and Christopher R. Vogel[1]

[1]Department of Engineering Science, University of Oxford, Oxford OX1 3PJ, United Kingdom; email thomas.adcock@eng.ox.ac.uk

[2]Oceans Graduate School, University of Western Australia, Perth 6009, Australia

Annu. Rev. Fluid Mech. 2021. 53:287–310

The *Annual Review of Fluid Mechanics* is online at fluid.annualreviews.org

https://doi.org/10.1146/annurev-fluid-010719-060207

Keywords

tidal energy, hydrodynamics, multiscale

Abstract

Placing mechanical devices into fast-moving tidal streams to generate clean and predictable electricity is a developing technology. This review covers the fundamental fluid mechanics of this application, which is important for understanding how such devices work and how they interact with the tidal stream resource. We focus on how tidal stream turbines and energy generation are modeled analytically, numerically, and experimentally. Owing to the nature of the problem, our review is split into different scales—from turbine to array and regional—and we examine each in turn.

1. INTRODUCTION

Hydrofoil: cross-sectional shape of a rotor blade that generates lift

Generating clean and predictable power is one of the key global challenges of the twenty-first century. Because options for clean power are dependent on the availability of local resources, a range of solutions are likely to be required to meet demand and climate change objectives. Tidal energy is a clean and predictable source of renewable energy. At present the use of this resource is limited, with current worldwide power production, mostly from tidal range facilities, around 500 MW. Power generation from tidal stream technology is expected to be several hundred megawatts once the first large tidal turbine farm, the MeyGen project in Scotland, is completed.

Power extraction from the tides dates back to medieval tide mills. Numerous proposals and theoretical developments were made in the twentieth century, with the largest developments being the La Rance Tidal Power Station (Brittany, France) and Siwha Lake Tidal Power Station (Gyeonggi Province, South Korea), opening in 1966 and 2011, respectively. There are several approaches to extracting power from the tide. Tidal barrages separate the open ocean from an impounded area of water. By periodically isolating the impounded region, a difference in head develops across turbines from which power may be generated when the impounded water is released. This approach has a relatively large environmental impact, and so engineers have also developed an alternative approach, which places a mechanical device, typically a turbine, into fast tidal streams. This review looks at this second approach; a review of tidal barrage technology is given by Neill et al. (2018).

There are many technical and engineering challenges that need to be mastered for tidal stream energy to deliver significant contributions to local or national power generation. These include practical issues of survivability and maintenance, in addition to financial, legal, and environmental issues. However, the most fundamental problem is how to turn the movement of the oceans due to the tide into a motion that can be used to turn a generator. Much of this challenge is one of understanding and modeling the fluid mechanics of the problem and this is the focus of the present review. Other reviews of aspects of tidal stream energy have been covered in articles by Garrett & Cummins (2008), Rourke et al. (2010), and Vennell et al. (2015), as well as in books by Greaves & Iglesias (2018) and Neill & Hashemi (2018).

This review starts with an overview of how power is extracted from tidal streams. Consideration of these fundamentals suggests a multiscale fluid mechanics problem. It is therefore convenient and scientifically appropriate to divide the problem according to nested length scales (device, array, and regional), which can then be considered separately.

2. FUNDAMENTALS

Practically generating energy from a fast tidal stream requires a motion to be induced in a mechanical device, which can then be used to drive a generator. There are a wide range of mechanisms that can be used to do this, but the most efficient has been to use the flow to generate lift on a moving hydrofoil. The hydrofoil must sweep a cross section of the flow.

A key idea is that a tidal turbine will apply a resistance to the flow over the area swept by the turbine blades. This will slow the flow passing through the turbine, while locally some flow will bypass the swept area. This idea leads to what is perhaps the simplest representation of a turbine: the classic actuator disc model. Actuator disc theory was first applied to wind turbines independently by Lanchester, Betz, and Joukowsky (van Kuik 2007). This model has formed the foundation for the most recent theoretical modeling of tidal turbine arrays. In its simplest form, the actuator disc model replaces the blades of a turbine with a permeable disc that provides a uniform retarding force across its area. This avoids complex flow structures around the individual turbine blades, but retains the important link between the net resistance offered by the turbine

and the bulk flow. Using control volume arguments, we can find the power, P, extracted by an actuator disc to be

$$\frac{P}{1/2\rho U^3 A} = C_P = 4\alpha^2(1-\alpha), \quad 1.$$

where α is the flow velocity fraction at the disc relative to the upstream velocity U, ρ is fluid density, and A is the cross-sectional area of the disc. The parameter α is necessarily less than one because a turbine can only retard the local flow. An important characteristic of Equation 1 is that the power coefficient has a maximum at $\alpha = 2/3$, for which $C_{P,\max} = 16/27$. This maximum, traditionally known as the Betz limit, identifies an optimum disc resistance (or blade properties and rotation speed) to generate energy. Larger resistance results in too much flow bypassing the disc, and lower resistance does not provide enough force to generate optimum power.

The Betz limit has proven to be a useful upper bound for wind turbine developers, with actual turbines producing slightly less power due to losses not accounted for in the classical model (Sørensen 2011). Garrett & Cummins (2007) first showed that the Betz limit needs to be corrected for in tidal turbines because tidal flows are bounded by the free surface and seabed. This results in a blockage, which helps to resist bypass flow and therefore increase power extraction. For a blockage B, Garrett & Cummins (2007) showed the following:

$$C_{P,\max} = \frac{16}{27}\left(\frac{1}{1-B}\right)^2. \quad 2.$$

Thus, the blockage is an important characteristic of a tidal stream turbine. This has important implications for device and array scale considerations, which are discussed further below.

Tidal stream turbines will only be feasible in locations where energy is sufficiently concentrated. This generally occurs where the geometry of coastlines leads to contraction of the flow and hence increased velocity. This has implications for device and array scales, as discussed below. Examples are shown in **Figure 1**. For the power density to make energy extraction feasible, typically the tidal range, and hence the head driving the flow, will also have to be large. Thus, candidate sites will typically be dominated by semidiurnal tides. Exceptions to this are archipelagos like Indonesia, Japan, or the Maldives, where the small gaps between islands experience strong flows even though the tidal amplitudes are relatively modest.

The force that generates the tide comes from the gravitational attraction of the moon and sun coupled with the relative rotation of the earth. This time-varying force generates oscillations

Power coefficient: $C_P = \frac{P}{1/2\rho U^3 A}$, the proportion of upstream kinetic flux that can be turned into useful power

Blockage: the area swept by the turbine blades relative to the cross-sectional area of the channel

Power density: power flux divided by a reference area; depending on the context this may be a horizontal or vertical area

Semidiurnal: a regime where there are roughly two high tides per day

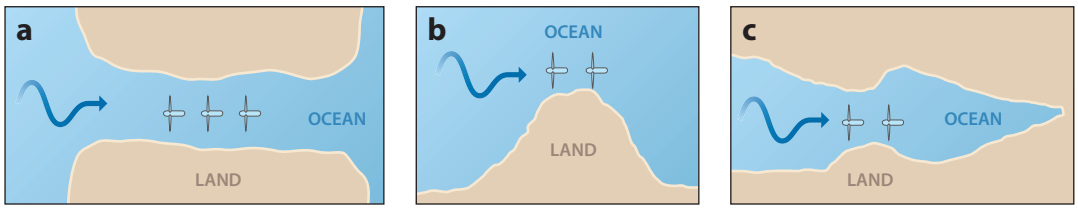

Figure 1

Some typical geometries of tidal energy sites with locations of turbines indicated. (*a*) Channel site. A channel connects two bodies of water with differing water levels. This drives a flow through the channel. Examples include the Pentland Firth, Scotland, and the Larantuka Straits, Indonesia. (*b*) A headland site. The strong current is usually caused by a combination of the head difference across the headland and a strong flow along the coastline being concentrated around the headland. An example is the Alderney Race off the coast of Normandy, France. (*c*) A basin site. These occur where there is an exceptionally large tidal range that drives a large flow. An example is the Minas Passage in Nova Scotia, Canada.

in the deep ocean basins, which in turn generate waves that travel up over the continental shelf (see, for example, Hendershott & Munk 1970, Pugh 1987). These tidal waves may be amplified at different locations by resonances and interactions as the waves pass around land masses.

Continental shelf: the relatively shallow-depth (<1,000 m) ocean near the coast

Axial-flow turbine: devices in which the axis of rotation is aligned with the flow direction

Cross-flow turbine: devices in which the axis of rotation is perpendicular (either vertical or horizontal) to the flow direction

Rated power: a turbine's maximum power output

One of the key engineering problems associated with tidal energy concerns the range of length scales involved. A regional model of the tides on one of the continental shelves of Europe will be on the order of 10^6 m, whereas in the boundary layers on the turbine blades, submillimeter resolution may be important. A further problem is that there are two-way interactions between these scales, although pragmatism requires that analyses of different scales be sometimes uncoupled. In the present review we have divided the problem into three scales based on the fluid physics involved, as described below.

(*a*) The device scale (10^{-3}–10^2 m) covers the working of an individual tidal turbine or a countable number of devices. In this we include the blade hydrodynamics and the flows around and downstream of the turbine. The support structure of the turbine and hydroelastic effects may also be important on this scale.

(*b*) The array scale (10^0–10^3 m) is appropriate for any analysis involving multiple turbines where the focus is on the hydrodynamics of the array and not on the large-scale tidal dynamics. In general, at this scale the number of turbines is large and not countable. At the array scale, the interactions between devices dominate the analysis.

(*c*) The regional scale (10^2–10^5 m), the largest scale we consider in this review, models the hydrodynamics of the tides and tidal streams. Tidal stream turbines, or at least the thrust from tidal stream farms, should be represented at this scale, but usually with many simplifications.

3. DEVICE SCALE

There are a variety of technological solutions to generate mechanical work from moving tidal streams. Conventional turbine types include axial-flow (propeller type) and cross-flow devices. Other device types build on these basic concepts with the use of, for instance, flow augmentation through ducts and flying wings on which turbines are mounted to develop greater relative velocities and higher power densities at the plane of extraction. The dynamic pressure in tidal flows is an order of magnitude greater than in wind flows, which results in significantly higher loading of rotors, necessitating sturdier blades that have greater spanwise flows and tip losses. Together with flow unsteadiness in the marine environment, this leads to differences in the designs of tidal rotors and wind rotors.

To date almost all turbines deployed and grid connected have been of the axial-flow variety and consist of two or more blades. Device sizes have been up to 18 m in diameter, working in flow speeds of up to 5 m/s, and with rated powers ranging from a few hundred kW to 1.5 MW. Devices range in complexity from simple fixed-pitch variable-speed devices (e.g., Schottel) to more complex variable-pitch and -speed devices that resemble modern wind turbines (e.g., SIMEC Atlantis AR1500). Turbines can be bottom mounted or deployed from floating platforms, with both solutions allowing for a single turbine or multiple turbines per structure.

Many of the decisions around device architecture stem from the flow environment and ensuing fluid mechanics. While average tidal flow speeds and directions are largely predictable, tidal stream turbines encounter a complicated flow environment due to the interactions of a sheared tidal flow, wave-induced velocities, and turbulent structures due to islands or seabed roughness and underwater features such as boulders. Additionally, turbines supported from floating structures may experience platform-motion-induced flows. These flow phenomena are illustrated in **Figure 2**. The tidal stream is vertically sheared with significant turbulence intensities of up to

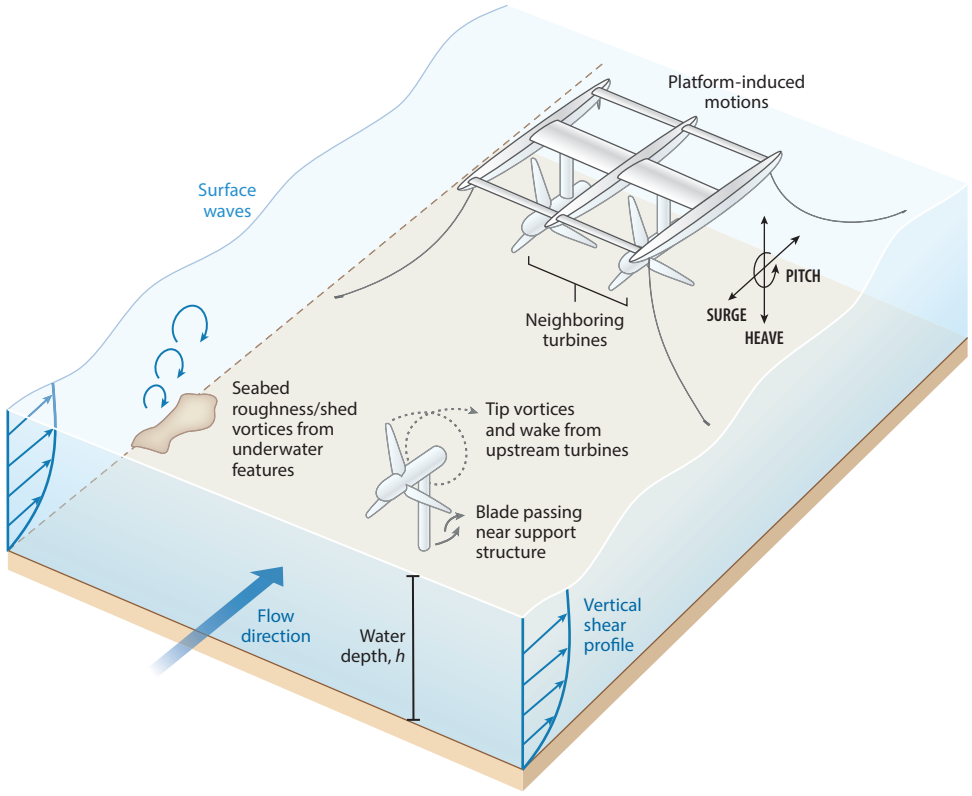

Figure 2

The flow environment and sources of important flow phenomena experienced by tidal stream turbines.

20% and structures with scales of tens of meters generated at the seabed (Greenwood et al. 2019). Waves generate significant loads and additional turbulence toward the free surface.

Field measurements have shown that the mean flow speed of a tidal stream varies with depth, resulting in a vertically sheared flow profile (Greenwood et al. 2019). The vertical profile is a function of the seabed roughness, which varies from site to site and may vary with flow direction depending on local bathymetry (Horwitz & Hay 2017). Free-surface effects, e.g., wind shear, can also reduce the flow speed as the free surface is approached (Stock-Williams et al. 2013). As the undisturbed kinetic energy flux scales with flow speed cubed, the majority of the tidal stream resource is found in the upper portion of tidal flows, which attracts device developers to shallower submersion depths. Although attractive to operate at the top of the water column, turbine loads scale with the square of flow speed. The upper portion of the water column is also subject to higher wave-induced velocities.

Devices must be able to operate across a range of flow speeds, potentially with hydrodynamic power capping, to protect drivetrain mechanical and electrical systems in order to withstand the large range of unsteady flow and extreme loading conditions. They must also be able to operate in both ebb and flood tides, requiring a degree of yaw control [e.g., MCT's (Marine Current Turbines) Seagen] or bidirectional capability (e.g., Nova Innovation). All of this must be achieved in a hostile environment in which inspection, maintenance, and recovery are difficult. There are different ways in which developers are trying to address these requirements, but two principal

Table 1 Summary of key parameters of prominent full-scale unducted rotors

	Number of designs	Rated power (MW)	Diameter (m)	Rated flow (m/s)	Approximate power coefficient, C_P	Pitch (Variable/fixed)
Large	7	1.0–1.5 (7)	13–21 (6)	2.65–3.0 (3)	0.37–0.42 (3)	5/2
Medium	3	0.5–0.6 (3)	16.5–18 (2)	2.3–2.4 (2)	0.31–0.43 (2)	2/1
Small	6	0.05–0.125 (6)	3–5 (6)	2.3–3.8 (6)	0.31–0.38 (5)	0/6

Information is incomplete: The number of devices for which information is available shown in parentheses. Some data (particularly C_P) are inferred from other data. Data in this table are from a variety of sources and should be used with caution.

technology bifurcations are emerging: larger devices that achieve scale through the size of device, and smaller devices that achieve scale through the number of devices. A summary of different rotors that have been developed is given in **Table 1**. Large, multi-megawatt high-technology devices are generally seabed mounted with speed and pitch systems allowing power rating and blade or nacelle reversal for yaw control. Small, sub-megawatt devices can be more readily mounted on multiturbine systems; have a simpler operation, with either fixed pitch with no power capping or, alternatively, stall control to limit power or hydroelastic blade deformation to relieve load; and have potentially bidirectional blades for simplicity of yaw control. Due to their smaller device size these devices are more amenable but not restricted to floating support systems.

Whether turbines are large or small or are built for axial flow or cross flow, the interaction with the steady and unsteady flow environment has similar features. Below we focus on axial-flow turbines, but much of the discussion applies to cross-flow turbines as well.

Turbine performance is typically characterized in terms of the thrust coefficient, C_T, and power coefficient, C_P. Typically, U is defined as the undisturbed flow speed at turbine hub height but may also be defined as an area-weighted average of flow speed over the rotor-swept area in a sheared flow. The turbine thrust and power coefficients are functions of tip-speed ratio and depend on the turbine operating strategy. Turbines that operate at a fixed rotation speed and a fixed blade pitch setting are mechanically simple but will operate away from the hydrodynamic optimum in many conditions. Variable rotational speed and variable blade pitch systems, as have been adopted for most large modern wind turbines, tend to be hydrodynamically more efficient, albeit with increased mechanical complexity.

Power capping: operating a turbine as a function of flow speed so that the rated power is not exceeded

Steady flow: flow that is not a function of time

Unsteady flow: flow that varies in some manner with time

Thrust coefficient: $C_T = \frac{T}{1/2\rho U^2 A}$, the ratio of turbine thrust per area to the upstream dynamic pressure

Tip-speed ratio: $\lambda = R\Omega/U$, the ratio of the circumferential speed, $R\Omega$, at the blade tip to the free-stream flow speed, U

Subcritical: flow velocities less than the shallow-water wave speed

Froude number: the velocity of the flow relative to the shallow-water wave speed

Chord: c, the dimension of a hydrofoil between the leading and trailing edges

3.1. Steady Loading

Tidal streams are subcritical open channel flows, with peak Froude numbers typically in the range of 0.1 to 0.2 (Vogel et al. 2016). Consequently, the free surface height drops and the downstream flow accelerates in response to energy extraction by turbines. Furthermore, tidal stream turbines typically occupy a more significant fraction of the available flow depth than wind turbines; thus, despite their outward similarities, there are several differences between wind turbine and tidal turbine fluid dynamics (Schluntz & Willden 2015). Nevertheless, the analysis of tidal stream devices has benefited from the models developed in the wind industry. The following provides a brief overview of loading on turbine blades (see also Burton et al. 2011).

Turbine blade geometry is typically described in terms of the radial distribution of chord, $c(r)$, and blade twist angle, $\beta(r)$. The blade profile typically transitions between thicker hydrofoil sections near the root to meet structural requirements to thinner hydrofoils further outboard for improved hydrodynamic performance (Grogan et al. 2013).

Figure 3 illustrates the relationship between the blade forces and the flow relative to a hydrofoil, $\mathbf{W}(r)$, which is made up of an axial-flow component, $\mathbf{U}_x$, which is reduced from the free-stream

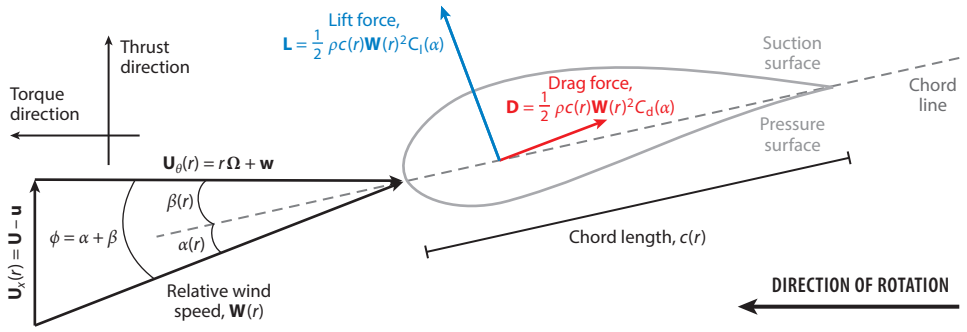

Figure 3

Illustration of the flow relative to a rotating hydrofoil at radius r from the turbine axis and the resulting lift (*blue*) and drag (*red*) forces. The blade is rotating toward the left.

flow speed U due to the turbine thrust, and a tangential component, $\mathbf{U}_\theta = \mathbf{\Omega} r + \mathbf{w}$, which is made up of the tangential speed of the blade at radius r and whirl velocity $\mathbf{w}$, which is induced to conserve the angular momentum of the flow. Lift and drag are functions of the angle of attack, $\alpha(r)$.

Turbine blade loads are often resolved into the thrust (axial) and torque-generating (rotational) directions. Two-dimensional (2D) blade element theory may be used to describe the spanwise components of a blade's thrust $\mathbf{T}(r)$ and torque $\mathbf{Q}(r)$ per unit span as

$$\mathbf{T}(r) = \frac{1}{2}\rho c(r)\mathbf{W}(r)^2 \left[C_l(\alpha)\cos\phi + C_d(\alpha)\sin\phi\right], \quad 3.$$

$$\mathbf{Q}(r) = \frac{1}{2}\rho c(r) r\mathbf{W}(r)^2 \left[C_l(\alpha)\sin\phi - C_d(\alpha)\cos\phi\right]. \quad 4.$$

While 2D theory provides a good description of the spanwise variation of thrust and torque along most of the blade, adjustments are required to account for the three-dimensionality of the flow in the tip and hub regions of the blade. The form of these corrections depends on the modeling approach used to describe the turbine. High-fidelity blade-resolved simulations directly resolve the flow around the blades, thereby enabling blade forces to be directly extracted from the simulations (Hansen & Johansen 2004). Lower-fidelity actuator models reduce computational costs by representing the forces imposed by the blades without requiring their direct resolution. Actuator disc models are an azimuthally averaged steady flow turbine representation where either the rotor thrust is prescribed, usually as a function of the dynamic pressure at the rotor plane, or the averaged blade forces calculated using 2D blade element theory are imposed on all the fluid passing through the rotor-swept area. Corrections are required to account for the disc representation of the turbine (for example, Glauert 1935), which accounts for finite blade number and tip vortex downwash.

Alternatively, actuator line models provide a reduced-order unsteady representation in which the blades are modeled as rotating momentum source lines along which blade forces are imposed on the flow. Corrections for 3D effects are applied to adjust the imposed forces in the blade root and tip regions; corrections may be isotropic (Shen et al. 2005) or anisotropic (Wimshurst & Willden 2017). As the blade tip is approached, 3D flow effects act to reduce the blade lift and increase its drag, resulting in aft rotation of the load vector (Wimshurst & Willden 2018). The higher level of loading experienced by tidal rotors, relative to wind rotors, results in more significant loading changes in the outboard sections. The various correction methods discussed herein

Blade twist angle: β, the angle between the chord line and the direction of blade travel

Angle of attack: $\alpha(r)$, the angle between the hydrofoil chord line and the incident flow vector, $\mathbf{W}(r)$

have been drawn from experience in the wind industry, and the effects of blockage, for example, on the accuracy of the correction methods, have yet to be demonstrated.

Cavitation: the formation and collapse of vapor bubbles due to pressure changes

Drawing on experience in aircraft design, blade tip modifications such as winglets have been proposed to suppress tip vortices and boost the production of lift (Ren et al. 2017). However, winglets can also increase parasitic drag and the increased structural requirements to support the winglet need to be balanced against the recovered power. Young et al. (2019) conducted a numerical and experimental study on winglet design, finding that pressure-side winglets provided better performance than suction-side winglets. However, optimal winglet design is closely related to blade geometry, and further work is required to understand the effect that winglets have on blade flows.

The uplift in turbine performance due to blockage effects was introduced in Section 2. Experimental (Ross & Polagye 2020) and numerical (Schluntz & Willden 2015) studies have shown that the change in turbine performance is appreciable when blockage exceeds 5%. At the device scale, increasing the blockage ratio results in increased resistance to bypass flow acceleration. At a given rotational speed $\mathbf{\Omega}$, the axial-flow speed at the rotor plane $\mathbf{U}_x$ will be greater with increased blockage ratio (Wimshurst et al. 2018), increasing the magnitude of the incident flow, $\mathbf{W}(r)$, and the angle of attack, α. This has two consequences: The lift and drag forces, and thus turbine thrust and torque, increase, and the angle of attack moves away from the design condition, reducing the lift-to-drag ratio along the blade. The first result means that turbines deployed in confined flows experience higher loads than their unblocked counterparts, which must be accounted for when analyzing the turbine's structural requirements (Vogel et al. 2018). The second result means that the rotational speed or the blade pitch angle need to be adjusted to target the design angle of attack along the blade in order to maximize rotor performance at higher blockage ratios. The increased thrust on the turbine as blockage increases results in a streamwise pressure drop, which equates to the pressure drop in the accelerated turbine bypass flow.

The hydrodynamic loads experienced by the blades can result in blade deformations in the flapwise (thrust), edgewise (torque), and twist directions based on the structural properties of the blade (Zilic de Arcos et al. 2019). There is feedback between the changes in blade geometry and the hydrodynamic loads leading to those changes. Blades tend to have high structural stiffness in the edgewise direction, resulting in negligible deformation (Grogan et al. 2013). However, deformations can be more significant in the flapwise direction, which may create additional spanwise flows along the blade, challenging the assumption of two-dimensionality of flows and forces along much of the blade. Geometric twist deformations result in a change in angle of attack, leading to changes in the lift and drag forces. Preconing is commonly employed in modern wind turbines so that as the blades bend backward under load they reach the designed (planar) conditions under maximum load.

The efficiency of axial-flow turbines is generally improved by designing for high tip-speed ratio, which also reduces the maximum drive train torque loads (Ning & Dykes 2014). However, operating turbines underwater requires the additional consideration of cavitation, which can cause significant damage to blade surfaces and thus the hydrodynamic performance of a tidal turbine. This is particularly significant for turbines high in the water column.

Although it is difficult to predict the precise onset of cavitation, the static pressure falling below the vapor pressure of the fluid is a precondition (Batten et al. 2006). As the static pressure increases with depth, this cavitation most likely occurs on the suction surface when the blade is in the top center position. However, the reduction in the magnitude of the pressure distribution associated with tip-loss effects means that the lowest static pressure on the blade occurs slightly inboard of the blade tip at about 95% span (Wimshurst et al. 2018). As the pressure distribution around the blade

depends on the rotational speed of the blade, the speed of rotors must be restricted (maximum design tip-speed ratio is usually around 5) especially for rotors passing close to the water surface so as to avoid cavitation. Alternatively the submersion depth of the turbine may be increased in order to permit higher design speeds, presenting an advantage to bottom-mounted devices with significant surface clearance. Hydrofoil sections may be chosen specifically with lower, more distributed suction peaks so as to minimize cavitation risk (Batten et al. 2006).

3.2. Unsteady Loading

Tidal stream turbines may encounter unsteady flows from several sources. Some sources of unsteady blade loads are deterministic, such as the periodic fluctuations due to the vertical shear profile and flow misalignment due to yaw, the blade passing the support tower, and the blade passing near flow boundaries or neighboring turbines. Other sources are stochastic, such as those due to wave-induced velocities, turbulent eddies, and, for floating turbines, platform-induced motions (Scarlett et al. 2019). Sequeira & Miller (2014) described the parameter space of unsteady loads on tidal turbines in terms of the unsteady flow frequency normalized by the mean flow blade-passing frequency, $k = \omega c/W$, and the nondimensional velocity fluctuation amplitude, $\eta = \Delta u_x/U_x$. As shown in **Figure 4** for the mid-span of a blade-mounted turbine, wave-induced unsteady velocities are predominantly low frequency and may be approximated as a quasi-steady fluctuation in load under some conditions, whereas seabed turbulence can be very high frequency but is typically of small amplitude. For turbine blades that pass near the surface, wave-induced velocities may be more important, and further consideration of dynamic loading effects may be required.

Unsteady flows contribute to both a change in the incident flow vector approaching the hydrofoil and a change in the hydrofoil coefficients. Under normal operating conditions, the incident flow vector $\mathbf{W}(r)$ is dominated by the rotational flow component $U_\theta(r)$ in the power-producing regions of the blade, so the change in magnitude of $\mathbf{W}(r)$ due to a gust is small. However, the flow

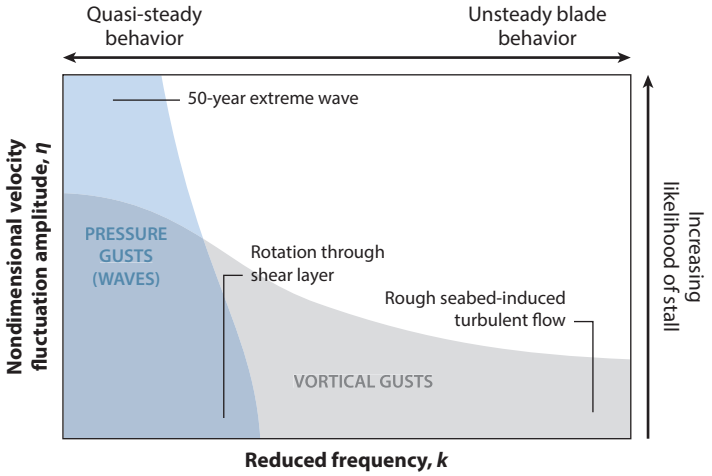

Figure 4

Parameter space of nondimensional amplitude, η, and reduced frequency, k, of unsteady blade flows for the mid-span of a tidal turbine blade. Figure adapted with permission from Sequeira & Miller (2014), copyright 2014 IEEE.

angle may change by several degrees, which can significantly affect the hydrofoil force coefficients. Following Burton et al. (2011), changes in turbine performance are largely driven by the changes in lift:

Added mass: a term in the dynamic equations related to the inertia of the fluid that must be accelerated when a body moves

$$\frac{\partial L}{\partial U} \approx \frac{1}{2}\rho c(r)\mathbf{W}(r)^2 \frac{\mathrm{d}C_L}{\mathrm{d}\alpha}\frac{\partial \alpha}{\partial U}. \quad 5.$$

There is a significant body of literature about the behavior of unsteady aerofoils, as summarized by Corke & Thomas (2015). Crucially, aerofoil/hydrofoil forces can depart significantly from steady 2D predictions. The change in performance varies with the angle of attack excursion, and the effect on blade loads can be significant, with loads exceeding the quasi-steady value by over 25% in model experiments (Milne et al. 2016).

Deterministic sources of blade loading variations include the vertical shear of the tidal flow and tower-passing perturbations (Ahmed et al. 2017). The vertical shear profile means that the axial component of $\mathbf{W}(r)$ varies with depth; thus, the flow angle ϕ is greater when the blade is in its uppermost position and smallest in its lowermost position. Similarly, the presence of the support tower reduces the axial-flow speed, perturbing the incident flow vector as the blade passes. The impact of the tower on flow speed can be evaluated using potential flow theory when the blade is upstream of the tower, but empirical models are required to account for separated flow if the blade is downstream (Burton et al. 2011). In a similar manner, periodic load fluctuations may also occur if the blades pass close to flow boundaries or neighboring turbines (McNaughton et al. 2019).

Stochastic sources of unsteadiness in the flow result in load fluctuations across a wide range of frequencies (Ahmed et al. 2017). Spectral peaks are associated with features such as channel bathymetry and underwater objects (Milne et al. 2016). Free-stream turbulence has the effect of spreading the spectral energy content of blade loads between the low frequencies associated with phenomena such as tower passing and the high frequencies associated with blade-generated turbulence (Ahmed et al. 2017). While the contribution of turbulence to mean turbine performance is small, it does increase the amplitude of load fluctuations (Afgan et al. 2013, Ahmed et al. 2017) and may also result in hysteresis of blade load curves due to the phase lag between blade forces and velocities (Milne et al. 2015, Scarlett et al. 2019). Turbulence may increase the peak root bending moment by up to 15% when the flow remains largely attached to the blade, with even greater increases in loads when separation and stall occur (Milne et al. 2016).

Surface waves result in velocity perturbations that are a function of wave frequency and decay with depth. These cause load fluctuations particularly for turbines deployed near the water surface. Data from the European Marine Energy Centre showed that wave-induced motions propagated to a depth of 20 m in 45 m of water depth (Norris & Droniou 2007). As wave-induced velocities decay with depth, the effects of waves on blade loading will likely interact with the shear profile to produce a temporally and spatially varying inflow (Sequeira & Miller 2014). An exception to this is very long period waves, which result in velocity perturbations that are almost uniform across the rotor-swept area.

Platform-induced motions have a similar impact on unsteady turbine loads. Surge oscillations result in velocity perturbations that are uniform across the rotor (Zhang et al. 2015), whereas platform pitching motions create a spatially varying velocity perturbation. Turbine blades may temporarily stall under large platform motions, which tend to reduce the mean thrust and power compared to the nonoscillating case and significantly increase fatigue loads (bin Osman et al. 2019). The added mass of turbines oscillating in surge has been found to be modest (Whelan et al. 2009, bin Osman et al. 2019).

3.3. Wakes

The dynamics and evolution of turbine wakes are important factors in planning tidal turbine farms. Wakes have an impact on the performance of downstream turbines and energy dissipation due to wake mixing. Turbine wakes are often divided into near- and far-wake regions.

Basin efficiency: the ratio of power usefully extracted by a turbine to the total power, including mixing losses, removed from a tidal flow

The near-wake region is strongly influenced by turbine geometry and the presence of coherent tip vortex structures, which break down within a few rotor diameters of the turbine (Chamorro et al. 2015). The near-wake region may also be influenced by the presence of the support structure. Experiments have demonstrated that the turbulence immediately downstream of the rotor is greatest near the blade tips (Mycek et al. 2014a, Stallard et al. 2015) and that wake structure is anisotropic due to the rotation imparted by the turbine (Chen et al. 2017). Stallard et al. (2015) reported that near-wake mixing started around one diameter downstream of the rotor, with the wake expanding as it propagates downstream, although differences between the vertical and horizontal confinement typical of tidal flows result in anisotropic wake expansion.

The far-wake region is characterized by a more generalized reduction in the momentum of the flow and is often described with a self-similar velocity profile (Stallard et al. 2015). Tip structures have started to break down at this stage. Evolution of the far wake is driven by the ambient turbulence levels and the blockage ratio. Ambient turbulence has been shown to have a significant impact on wake evolution, particularly in the far-wake region, due to its effect on the exchange of momentum between the ambient flow and the wake (see, for example, Mycek et al. 2014a, Chamorro et al. 2015). Turbulence levels vary across tidal sites, with intensities of up to 20% reported (Thomson et al. 2012, Mycek et al. 2014a). These are higher than that for offshore wind and lead to faster wake recovery. Coherent flow structures play a more important role in wake recovery than simply increasing the ambient turbulence level and have been observed experimentally to be more effective at enhancing tip vortex breakdown, resulting in accelerated wake recovery (Chamorro et al. 2015). Blockage due to the greater shear that develops between the wake and the accelerated bypass flow also has an effect on the wake recovery and, thus, the mixing (Chen et al. 2017).

Numerical simulation is used more widely than experiments to investigate the evolution of turbine wakes. However, simulations must be performed carefully to accurately simulate sources of turbulence and wake evolution. While Reynolds-averaged Navier–Stokes (RANS) and large eddy simulation (LES) studies can yield close agreement with predicted turbine power and thrust, LES modeling is required to capture information about unsteady loading and resolve and propagate wake structures such as tip vortices (Afgan et al. 2013). RANS models tend to overestimate eddy viscosity in the wake region and therefore overstate wake recovery. Shives & Crawford (2016) demonstrated that RANS turbulence models with tuned coefficients, or RANS models that limit the eddy viscosity in the wake region, are in better agreement with experimental observations of wake recovery.

Mixing of the wake and bypass flows necessarily results in energy dissipation, which must be accounted for within overall energy budgets. The precise mechanics of wake evolution are less important at the array and basin scale than an estimate of the power lost in the wake-mixing processes, which can be described using the concept of basin efficiency (Belloni et al. 2013).

3.4. Interference Effects

Beneficial and detrimental impacts on turbine performance have been observed depending on the mechanism of turbine–turbine interference. Close lateral spacing of turbines can lead to increased turbine power, whereas turbine wakes negatively impact the performance of downstream turbines.

Mycek et al. (2014b) conducted experiments of two turbines aligned in the streamwise direction over a range of interturbine spacings. Significant reductions in power (50% or greater) were observed for the downstream turbine in low–ambient turbulence levels, whereas smaller reductions in power (15%) were recorded at higher levels of turbulence intensity. Although ambient turbulence leads to increased load fluctuations for a turbine, it can have significant benefits for downstream turbines due to the faster recovery of the wake upstream. The importance of wake effects on downstream turbine performance is also a significant area of research in wind energy (Stevens & Meneveau 2017).

Uniform flow: flow that has a spatially and temporally uniform velocity profile

Global blockage: the swept area of all turbines divided by the total cross-sectional area of the channel

Local blockage: the swept area of a single turbine divided by the cross-sectional area of the flow passage encompassing the device

The mechanism by which blockage affects turbine loading has been established. Close lateral positioning of turbines relative to the oncoming flow can be utilized to amplify blockage effects and boost turbine performance through constructive interference effects (McNaughton et al. 2019). Here, neighboring turbines act to restrict the free expansion of the turbine streamtube, which enables each turbine to present a higher thrust and maintain a higher mass flux through it, resulting in performance gains. While increased blockage can lead to improved turbine performance, fully exploiting the performance gains available through constructive interference requires that the turbines are designed to target optimal operating conditions in the closely spaced environment (Schluntz & Willden 2015, Cao et al. 2018). McNaughton et al. (2019) demonstrated experimentally using two 1.2-m-diameter rotors that a ∼20% uplift in power was realizable, with an accompanying ∼8% increase in thrust, by designing turbines to exploit constructive interference effects.

The flow approaching fences of small numbers of turbines will likely vary across the turbines due to spatially varying flow conditions, as well as the interactions between device- and array-scale flows, as discussed further in Section 4. Cross-fence variations in approach flow have been observed numerically (Vogel & Willden 2017) and experimentally (Cooke et al. 2015) and have resulted in cross-fence variation in turbine performance. Turbines may be operated differentially across the fence, either through pitch control or by varying rotational speed, to mitigate such cross-fence variations, although this is likely to be detrimental to the maximum achievable power of the turbine fence. However, simulations suggest that significant reductions in turbine thrust can be made for only modest reductions in fence power (Vogel & Willden 2018).

The performance benefits of constructive interference occur below rated flow speed, as turbine power is capped to a constant level when the tidal current exceeds this speed. Constructive interference effects on turbine loads may diminish above the rated flow speed if pitch-to-feather control is used, as turbine thrust and consequently the impact of turbines on the tidal flow are reduced at high flow speeds (Vogel & Willden 2018).

4. ARRAY SCALE

Research at the array scale has focused primarily on understanding the interactions between a large number of turbines placed in close proximity. Several key questions arise at this scale, including how to arrange turbines and how best to operate them to generate energy efficiently. Answering these questions requires the development of models that can resolve a large number of turbines and capture interactions between them.

4.1. Arrays in Shallow Uniform Flow

If it is reasonable to assume that an array will be placed in shallow, uniform flow, actuator disc theory can be extended in several ways to theoretically investigate turbine arrays. Nishino & Willden (2012), for example, introduced the concept of scale separation to analyze a partial row of tidal

turbines using actuator disc theory. They assumed that each turbine within the row could be modeled using an actuator disc with a local blockage defined by the spacing between turbines. At the array scale, the collection of turbines in the row could be thought of as a second actuator disc. The local and array scales were linked by ensuring consistency of force and velocity across the scales. For a small array (global blockage tending to zero) in a wide channel, Nishino & Willden were able to show that the maximum power that could be extracted by turbines in a row is $C_{P,\max} = 0.798$ provided the local turbine blockage is ∼0.4.

Despite the simplicity of the Nishino & Willden model, several numerical simulations of porous discs have been found to give good agreement, but only if the number of turbines in the row is large (Nishino & Willden 2013, Perez-Campos & Nishino 2015). Experiments of model-scale turbines and porous discs have shown qualitative agreement with the theoretical model (Cooke et al. 2015).

Building on the work of Nishino & Willden, Cooke et al. (2016) suggested that the idea of scale separation need not stop with just two scales. They showed that if a third scale were permitted (representing subrows within a partial row), more power could be extracted ($C_{P,\max} = 0.865$). This increase is realized theoretically because a higher blockage can be achieved at the smallest scale, resulting in more efficient energy extraction. In fact, the idea can be generalized to n scales, for which it can be shown numerically that $C_{P,\max}$ approaches unity as n tends to infinity in an infinitely wide channel. The number of turbines must be large for this result to be realized.

Extension of these actuator disc models to multirow arrays requires some way to arrange turbines behind each other. Draper & Nishino (2014) introduced a model to capture two discs arranged in either a centered or a staggered arrangement in a uniform flow. This model was then combined with an argument of scale separation to investigate arrays comprised of two rows of centered or staggered turbines. Draper & Nishino's analysis permitted a theoretical ranking of different multirow arrangements of turbines and showed that, for an array of N identical turbines, one row of closely spaced turbines ranks best, followed by staggering the turbines across two rows, which is better than two rows of centered turbines (**Figure 5**). The relative benefit of adopting a single row of turbines compared with a staggered arrangement is consistent with that found in simulations of uniformly porous discs (Hunter et al. 2015), and the conclusion that staggered arrays outperform centered arrays is consistent with Divett et al.'s (2013) numerical results.

Despite the interesting insight that can be gained by these models of actuator disc arrays, it is important to note some key limitations. Firstly, the models do not properly represent wake flows, and so any model with centered turbines is likely to be qualitative at best. Empirical models that employ wake superposition may have more quantitative promise (e.g., Stansby & Stallard 2016). The actuator disc models also ignore blade-scale processes and the effects of turbine interactions on these processes (as discussed in Section 3), as well as free-stream turbulence, which enhances wake mixing.

In addition to these limitations, the actuator disc models ignore variations in the upstream velocity profile and the influence of background effects such as bottom friction, local changes in seabed bathymetry, and flow acceleration. The interaction between arrays and larger-scale tidal dynamics is also important, as discussed below in Section 5.

4.2. Arrays in Unsteady, Frictional, and Nonuniform Flows

All tidal flows are time varying and often occur in sufficiently shallow water for bottom friction to play an important role in the tidal dynamics. Garrett & Cummins (2013) were the first to show how both acceleration and bottom friction influence flow through a porous structure (in their

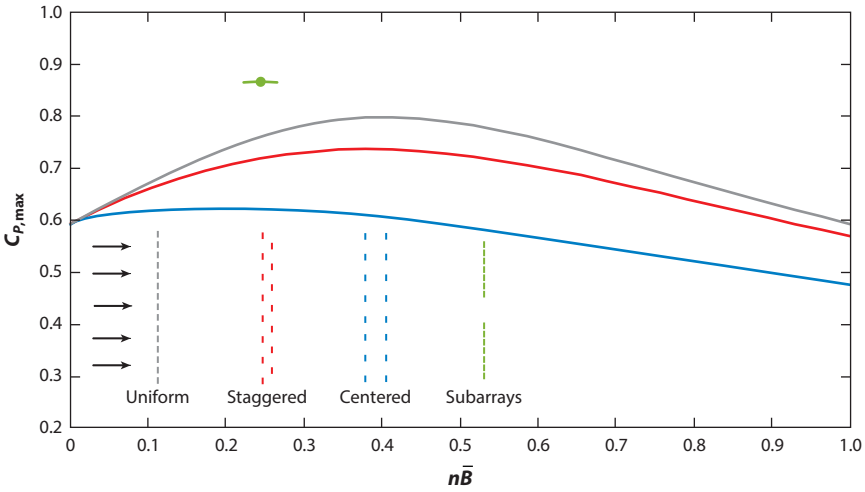

Figure 5

Theoretical prediction of maximum power coefficient, $C_{P,\max}$ for different turbine arrangements. The horizontal axis is equal to the number of rows, n, multiplied by the mean blockage per row, $\bar{B}$. This ensures that the number of turbines is consistent across the arrangements, since the blockage per row in the centered and staggered arrangements is one half of that in a uniform row if the number of turbines is fixed. For the subarray, only the peak value is shown at a mean blockage that accounts for the spacing of the turbines and subarrays.

case, a horizontal, circular patch). Both acceleration and bottom friction were shown to inhibit bypass flow around the patch, thus providing greater energy potential. For a steady flow with bed friction, Creed et al. (2017) replaced the circular patch with a partial row of turbines, enabling a direct link between bottom friction and local turbine spacing. This showed that turbines may be spaced more closely than predicted by the frictionless model. Bonar et al. (2019) considered a partial row of turbines in a channel with background friction and an accelerating flow. Their work goes beyond that of Creed et al. (2017) to demonstrate that both acceleration and friction influence optimal turbine spacing, suggesting that tidal array optimization is quite complex and that one cannot completely separate the array scale from the larger resource scale. However, Bonar et al.'s work also showed that for most sites with a realistic array, the effect of acceleration can be neglected.

The problem of nonuniform flow can, in principle, be treated with actuator models. However, theoretical models of arrays in nonuniform flow have yet to be developed. Nevertheless, Funke et al. (2014) introduced a promising numerical technique to optimize arrays in these situations using adjoint techniques. They used this approach to optimize the arrangement of arrays with each turbine modeled as a small patch of additional bed friction in a shallow-water model. These numerical methods have the potential to be extended to account for practical constraints on array layout, such as cable routing and nonuniform turbines (e.g., Culley et al. 2016).

5. REGIONAL SCALE

The basin scale looks at understanding the tide at a sufficiently large scale to predict the fast tidal streams and the impact of energy extraction on tidal hydrodynamics. The primary purpose of work at this scale is to determine and understand the magnitude of the resource and its characteristics.

The environmental impact is also often assessed at this scale. Tidal stream turbines will alter the physical environment, for instance, by changing sediment transport and pollutant dispersal, and these can have wider impacts on the marine environment. Energy extraction and environmental effects are coupled, and it may be that environmental limitations place a restriction on how much of the tidal resource can be exploited. The community is still at an early stage of understanding these issues and so they are not analyzed in detail here.

Atmospheric forcing: the force applied to the ocean by wind shear and pressure variations

Ocean currents: oceanic-scale and slowly varying currents such as the thermohaline circulation

Radiation stress: wind generated wave-induced momentum flux

5.1. Simplified Models

The simplest model at the regional scale was introduced by Garrett & Cummins (2005). It models a tidal channel driven by a time-varying head difference between two oceans (see **Figure 1*a***). By integrating in three spatial directions, the model reduces the problem to solving for one, time-varying flow rate. The model captures the leading-order physics of tidal energy extraction and is useful for simple numerical experiments and for providing some basic insights into different candidate sites.

The model simplifies to a nondimensional equation (see Garrett & Cummins 2005):

$$\frac{\mathrm{d}Q^*}{\mathrm{d}t} = \cos(t) - (\lambda_0 + \lambda_1)\, Q^* \,|Q^*|\,, \qquad 6.$$

where Q^* is a nondimensional flow rate. The parameter λ_1 relates the turbine thrust to the other forces in the channel. The parameter λ_0 describes the relationship between the drag forces and inertia forces in the channel: the dynamic balance. The dynamic balance of a candidate site indicates the dominant physics in the analysis even for locations that are not strictly channels. For a candidate site, this is most robustly determined from the phase lag between the water level difference across a site and the current.

The Garrett & Cummins channel model has been extended to look at other problems such as a bay connected to the ocean (Blanchfield et al. 2008) and to look at multiple interconnected channels (Cummins 2013, Draper et al. 2014). Other simplified models are useful for fundamental understanding at the regional scale. These include 1D shallow-water models (e.g., Rainey 2009) and resonance models (e.g., Arbic & Garrett 2010).

5.2. Modeling Real Sites

For a specific regional site, modeling must be carried out numerically. In regional-scale models, the dominant flows are driven by the gravitational pull of the moon and sun. However, unless the model is very large (e.g., covering much of an ocean), we can simply impose the incoming tidal wave on the edge of the domain, as the body force from the tide acting locally on the fluid on the continental shelf is relatively small. Typically, we may need to apply the water levels from only a few dominant tidal constituents, but this will be site specific. The size of the domain must be chosen with caution, as artificially extracting energy from the model can alter the tides on the boundary (Garrett & Greenberg 1977). In practice, as long as the additional power dissipated is small compared to the total energy dissipated by the model (i.e., the model is large relative to the turbine farm), imposing the naturally occurring tides is acceptable. Local atmospheric forcing and radiation stresses from waves might be important for determining extremes but are sufficiently intermittent that they can typically be ignored from resource assessments. Ocean currents are typically difficult to simulate accurately in small-scale models but in some areas might contribute significantly to the resource.

Shallow-water equations: a simplification of the Navier–Stokes equations based on depth averaging the flow

Wetting and drying: the phenomena whereby part of the numerical domain dries out or floods due to the rise and fall of water level

Coriolis term: the apparent deflection of a current on the rotating earth when viewed in an inertial frame of reference

To date, the vast majority of modeling at the basin scale is done by solving the 2D shallow-water equations (see Pugh 1987). These provide an excellent model for tidal hydrodynamics in the open ocean. They are relatively straightforward to solve numerically, although some aspects such as wetting and drying can complicate things, and computational efficiency is always a consideration. Although the shallow-water equations are a satisfactory model in the open ocean, it is unclear how accurately they model fast tidal streams (see, for example, Stansby 2006). In fast tidal streams, nonhydrostatic effects are likely to become important with strongly 3D flows in some areas. To capture this physics, one needs 3D models. Because of the complexity, at present layered models are generally used. Good results are starting to be achieved with such models (de Dominicis et al. 2017, O'Hara Murray & Gallego 2017, Thiébot et al. 2020a).

Validation against in situ measurements of currents is important when modeling real sites. The numerical models used generally have empirical factors (e.g., friction coefficient) that are necessary to fine-tune for different locations. This is necessary not only because of the physical simplifications of the models but also because, in general, the boundary conditions (e.g., exact bathymetry, seabed type, inflow turbulence) are not known accurately. Measuring currents is difficult, expensive, and noisy and generally only done at limited locations across a candidate site. The amplitude, direction, and phase (i.e., the time of peak flow) of the current all need to be examined. However, in our view, particular weight should be placed on examining the phase, as this is dependent primarily on the dynamic balance, described above, rather than on local factors, and thus is less susceptible to noise or measurement errors.

To our knowledge, the largest-scale laboratory experiments were conducted by Draper et al. (2013), and even in these, the effect of the inertia of the tidal flow was small. The fundamental experimental problem is the size of the facility required, given the much greater horizontal length scales involved compared to the vertical length scales—as the vertical length cannot become too small without nonrelevant physics dominating the flow. It is also difficult experimentally to apply boundary conditions and simulate effects such as the Coriolis term.

5.3. Representation of Turbines at the Basin Scale

A large array of tidal stream turbines are expected to apply sufficient thrust to the flow to significantly alter the hydrodynamics. Thus, these need to be represented in a model. It will not be possible to model detailed turbine physics at the basin scale, and it does not seem feasible to couple a computationally demanding numerical model for the turbine into a basin-scale model. Therefore, computationally fast low-order models need to be used. Analytical or semianalytical models are possible, such as actuator disc theory or constrained blade element models. Alternatively, parameterizations based on numerical or experimental results can be used.

A key issue for basin-scale models is how to apply the correct force to the flow to represent the thrust from the presence of turbines. Tidal stream turbines may also add turbulence, and in a 3D model the force should be applied at the right distance from the seabed, but generally these aspects are of secondary importance. The simplest method is to enhance the bed friction so as to either represent an array of turbines or try to represent individual turbines, although this usually requires some spatial smearing to keep the numerics stable. This is usually effective at applying the right amount of thrust to the model. However, behind a real turbine there will be energy dissipated in 3D mixing. This is where caution is required. At present, basin-scale models cannot properly resolve such wakes and there is often some uncertainty about what physics the model is capturing. Therefore, we suggest that it is preferable to explicitly not attempt to resolve the individual turbine wakes and instead account for the wake loss using an analytical correction (see Vogel et al. 2017). An alternative way of doing this is to impose an appropriate difference in water level across a turbine array, as introduced by Draper et al. (2010).

5.4. Turbine Operations: Basin-Scale Considerations

The control and design of tidal stream turbines will depend on the tidal hydrodynamics at a site. Some information from the basin scale (i.e., what flows the turbine will actually experience) should be fed into the design of tidal stream turbines.

In the wind industry, turbines are straightforwardly designed to maximize the power coefficient. Vennell (2010) argued that this is not the optimal strategy for tidal stream turbines, as they have a back effect on the speed of the tidal stream. If too great a thrust is applied by the turbines to the flow, the decrease in the energy of the flow outweighs the increase in kinetic efficiency. Vennell introduced the idea of tuning the turbines to a particular location so as to optimize the available energy. This has been applied to the analysis of real sites (e.g., Adcock et al. 2013) where it made a small difference to the power output. Vennell's (2010) work was extended in Vennell (2016) to consider time-varying turbine resistance. However, this work was primarily based on actuator disc models of turbine behavior. When more realistic models of tidal turbine characteristics are used, tuning becomes less significant and can generally be neglected (Chen et al. 2019). Thus, in practice, tuning may not be important and turbines can be designed to maximize the power coefficient.

Like wind turbines, tidal stream turbines will be designed to have a rated power that is somewhat lower than the rated power that would be needed to extract the maximum possible energy. The average flow is much less than the peak flow. It will not be feasible to extract all the power at spring tide, as this would give the system an uneconomically low capacity factor (Adcock et al. 2014, Vogel et al. 2019). Tidal turbines will be expected to power cap, the mechanics of which was discussed in Section 3. An improvement in capacity factor can be achieved for a small reduction in mean power. A small extra step is also to thrust cap, which limits the peak forces (and reduces environmental impact) on the turbine and its structure with only a small penalty in power (Wang & Adcock 2019).

Capacity factor: the power available for generation averaged over a long period of time divided by the rated power

5.5. Resource Assessment

One of the key purposes of modeling at the basin scale is to determine the tidal stream resource of a site.

The classical approach uses the naturally occurring (undisturbed) kinetic energy flux passing through a site or the swept area of a turbine farm (EMEC 2009). The flux is then usually multiplied by a factor of less than one to account for inefficiencies. This approach follows that of the wind industry, and kinetic flux is typically found from a numerical model. Most resource assessments in the literature use this method and it continues to be widely used. The kinetic flux approach has several clear disadvantages. Firstly, as pointed out by Garrett & Cummins (2005), there is no direct relationship between the kinetic flux and the tidal resource—this is partly because the presence of turbines will slow the flow from its natural state but also because it is possible to extract more power than the kinetic energy (Vennell 2013). A second disadvantage is that the kinetic flux is proportional to velocity cubed. Small inaccuracies in the velocity can lead to significant uncertainty in the estimate. Despite these key technical problems, for small arrays (where the disruption to the flow is minimal) this remains a useful technique for deriving estimates of the resource.

An alternative to analyzing the undisturbed kinetic flux is to include a resistance to the flow representing the presence of tidal turbines. The simplest step is then to calculate the extracted power, which is simply the energy dissipated by the resistance. This resistance can then be optimized to maximize the energy extracted. It is helpful to consider some limiting cases. If there is no artificial resistance to the flow, then no power is extracted. Similarly, if the resistance is so high

that there is no flow through the turbines, no power can be generated. There will be an optimum between these extremes. This approach was introduced by Garrett & Cummins (2005) and has been widely used (e.g., Karsten et al. 2008, O'Hara Murray & Gallego 2017). This method provides an upper bound on the resource since it does not account for energy loss in wake mixing, viscous effects on the blades, parasitic drag from the support structure, etc. Nevertheless this approach is less dependent on modeling assumptions than the kinetic flux approach and provides a well-defined upper bound on the resource.

To refine the upper-bound estimate of the tidal resource, there is a need to begin to link the dissipation to actual turbine arrays. Adcock et al. (2013) adopted actuator disc theory to represent rows of turbines within a numerical model of the Pentland Firth. With this representation they were able to separate the power removed by turbines from inevitable local wake losses, hence enabling the calculation of the available power to turbines as distinct from the total extracted power removed from the tidal flow. In the interpretation of their results, Adcock et al. (2013) noted that as additional rows of turbines are added to the model, there is a diminishing return and the power per turbine reduces. At some stage, the additional power from adding more rows would be too small to be worthwhile economically. Adcock et al. (2013) suggested that a refined upper bound on the resource could therefore be estimated by adding turbines until the power per swept area of the turbines fell below that of an offshore wind turbine. Of course, this argument was only an initial attempt to revise the resource based on economic arguments. There is room for refinement in the condition used to set the upper bound and in the model used to represent turbines within the model. For a range of scenarios, Chen et al. (2019) found that actuator discs overestimated the power by 60–70% relative to a more realistic model of turbine characteristics. Further reductions would result from support structure drag, power capping, and restrictions on the environmental impact.

Figure 6 helps to demonstrate the above approaches. Note that quantitative numbers will vary between sites (for instance, the peak of the extracted power curve may be less than one). The diminishing return can be observed as more rows of turbines are added.

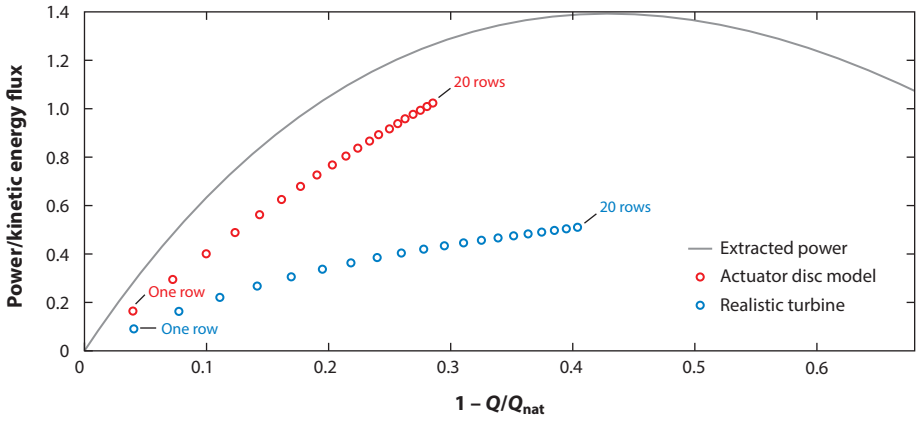

Figure 6

Typical power characteristics of a tidal site based on a site modeled with the Garrett & Cummins (2005) model with dynamic balance parameter $\lambda_0 = 1$, following also Vennell (2010). The power is normalized by the naturally occurring kinetic energy. Turbines have a blockage of $B = 0.2$ and extend across the channel. Realistic turbines are based on the model described by Vogel et al. (2018), with additional drag from the support structure. The power output is plotted against the nondimensionalized change in flow rate, $1 - Q/Q_{\text{nat}}$.

5.6. Predictability and Intermittency of Power Production

One of the advantages of tidal energy is that, in principle, it is predictable. The movement of the fluid is driven by the movement of the earth, sun, and moon, all of which are effectively known indefinitely far in advance. Atmospheric disturbances and changes to tidal patterns (e.g., by changes in bathymetry) would usually only have a minor effect on power production. There will be high-frequency fluctuations in power (Lewis et al. 2019), but these average out over timescales of the order of tens of minutes.

In practice, the methodology to predict fast tidal currents is imperfect. The standard method used for tidal prediction is harmonic analysis. The method works well for tidal predictions of water levels and offshore tidal currents. However, fast tidal currents are complex and harmonic analysis is an imperfect model (Godin 1970, Polagye et al. 2010). While harmonic analysis is still a good starting point, there is much scope for improving the temporal energy yield predictions.

Around a land mass with the same length scales as that of a tidal wave (hundreds or thousands of kilometers), the power will in general be out of phase between different sites. If several sites produce similar power, then this can smooth the overall power production (Neill et al. 2016). There may be some scope for controlling the timing of power production (see Vennell & Adcock 2014), but with a realistically sized array the thrust is sufficiently small that it is probably going to be marginal. However, while over a daily cycle different sites can smooth the overall power output over a longer period, there is a substantial variation in the power output. Longer tidal cycles, such as the spring–neap cycle, are dependent on the relative position of the earth, moon, and sun and therefore are in phase for all sites. These variations could be of the order of 10 in terms of theoretical power. There will also be interannual variations such as those with a period of the 18.6-year tidal cycle (Stock-Williams et al. 2013, Thiébot et al. 2020b).

Harmonic analysis: analysis of a tidal time history to extract signals at frequencies corresponding to known tidal constituents

Tidal constituent: a frequency at which it is expected that there will be a tidal oscillation due to a relative movement of astronomical bodies at that frequency

SUMMARY POINTS

1. There are now multiple grid-connected tidal stream turbines of different architectures providing renewable energy that have collectively delivered over 100 GWh. Understanding of the fundamental fluid mechanics has developed over the last 20 years, enabling better design of turbines and better assessment of available resources.
2. The tidal stream community has benefited greatly from knowledge transfer from the wind industry. There are, however, important differences in turbine design: The steady loading per unit area is more than an order of magnitude higher, and the environment is harsher due to higher turbulence and wave loading. Together with free-surface and blockage effects, these challenges have led to more robust designs for tidal rotor blades, and turbines more generally.
3. Tidal rotors can occupy a significant proportion of the water column and potentially the channel width, leading to important blockage effects. Blockage can increase turbine loads and potentially turbine performance if properly designed for, but it must always be accounted for in device modeling and design.
4. The tidal problem is more tightly coupled across scales than in wind, as the ratio of turbine thrust to channel-stream momentum is higher. This has led to the development of multiscale modeling approaches and associated multiscale performance limits. Such modeling approaches are now starting to find use in large wind farm modeling for which the thrust–momentum ratio has become more significant through the monotonic increase in turbine and farm size.

FUTURE ISSUES

1. Understanding and measurement of the flow environment is vital for the effective design and operation of tidal stream turbines and farms of turbines. Although flow measurements in the field are both difficult and expensive, measurement campaigns, together with developments to analysis techniques, will be required to deliver underpinning flow-field knowledge.
2. Unsteady loading of turbine blades, and its prediction, is a key problem, and even with better field and laboratory measurement of flow conditions, understanding how unsteady flow structures generate unsteady blade loading is nontrivial. Carefully designed experiments and simulations will be required to expose the fluid–structure interaction mechanisms.
3. Multiscale modeling must develop to include key interactional physics processes across scale boundaries. It is neither possible nor necessary to include all interactions, and modeling must focus on key physics as informed by simulation and measurement. There is commonality with wind farm modeling here, and a key issue for both wind and tidal power is better understanding and parameterization of device wakes and their interactions within array-scale models.
4. Validation at all scales is key to building confidence in understanding and engineering models, leading to reduced conservatism in design and operation. While some relatively small-scale and limited-device experimentation has been conducted, larger and more sophisticated turbine tests, as well as data from multiple turbine field deployments, are required to validate detailed and multiscale flow physics that have been postulated and thus far only simulated.

DISCLOSURE STATEMENT

The authors are not aware of any biases that might be perceived as affecting the objectivity of this review.

ACKNOWLEDGMENTS

R.H.J.W. is supported by an EPSRC (UK Engineering and Physical Sciences Research Council) Advanced Fellowship (EP/R007322/1).

LITERATURE CITED

Adcock TAA, Draper S, Houlsby GT, Borthwick AGL, Serhadloğlu S. 2013. The available power from tidal stream turbines in the Pentland Firth. *Proc. R. Soc. A* 469(2157):20130072

Adcock TAA, Draper S, Houlsby GT, Borthwick AGL, Serhadloğlu S. 2014. Tidal stream power in the Pentland Firth–long-term variability, multiple constituents and capacity factor. *Proc. Inst. Mech. Eng. A* 228(8):854–61

Afgan I, McNaughton J, Rolfo S, Apsley DD, Stallard T, Stansby PK, 2013. Turbulent flow and loading on a tidal stream turbine by LES and RANS. *Int. J. Heat Fluid Flow* 43:96–108

Ahmed U, Apsley DD, Afgan I, Stallard T, Stansby PK. 2017. Fluctuating loads on a tidal turbine due to velocity shear and turbulence: comparison of CFD with field data. *Renew. Energy* 112:235–46

Arbic BK, Garrett C. 2010. A coupled oscillator model of shelf and ocean tides. *Cont. Shelf Res.* 30(6):564–74

Batten WMJ, Bahaj AS, Molland AF, Chaplin JR. 2006. Hydrodynamics of marine current turbines. *Renew. Energy* 31:249–56

Belloni CSK, Willden RHJ, Houlsby GT. 2013. A numerical analysis of bidirectional ducted tidal turbines in yawed flow. *Mar. Technol. Soc. J.* 47(4):23–35

bin Osman MH, Willden RHJ, Vogel CR. 2019. The effects of surge motion on floating horizontal axis tidal turbines. In *Proceedings of the 13th European Wave and Tidal Energy Conference (EWTEC 2019)*, Pap. 1295. Southampton, UK: Tech. Comm. Eur. Wave Tidal Energy Conf.

Blanchfield J, Garrett C, Wild P, Rowe A. 2008. The extractable power from a channel linking a bay to the open ocean. *Proc. Inst. Mech. Eng.* 222(3):289–97

Bonar PAJ, Chen L, Schnabl AM, Venugopal V, Borthwick AGL, Adcock TAA. 2019. On the arrangement of tidal turbines in rough and oscillatory channel flow. *J. Fluid Mech.* 865:790–810

Burton T, Jenkins N, Sharpe D, Bossanyi E. 2011. *Wind Energy Handbook*. Chichester, UK: Wiley. 2nd ed.

Cao B, Willden RHJ, Vogel CR. 2018. Effects of blockage and freestream turbulence intensity on tidal rotor design and performance. In *Proceedings of the 3rd International Conference on Renewable Energies Offshore (RENEW 2018)*, ed. CG Soares, pp. 127–36. Boca Raton, FL: CRC

Chamorro LP, Hill C, Neary VS, Gunawan B, Arndt REA, Sotiropolous F. 2015. Effects of energetic coherent motions on the power and wake of an axial-flow turbine. *Phys. Fluids* 27:055104

Chen L, Bonar PAJ, Vogel CR, Adcock TAA. 2019. A note on the tuning of tidal turbines in channels. *J. Ocean Eng. Mar. Energy* 5(1):85–98

Chen Y, Lin B, Lin J, Wang S. 2017. Experimental study of wake structure behind a horizontal axis tidal stream turbine. *App. Energy* 196:82–96

Cooke SC, Willden RHJ, Byrne BW. 2016. The potential of cross-stream aligned sub-arrays to increase tidal turbine efficiency. *Renew. Energy* 97:284–92

Cooke SC, Willden RHJ, Byrne BW, Stallard T, Olczak A. 2015. Experimental investigation of tidal turbine partial array theory using porous discs. In *Proceedings of the 11th European Wave and Tidal Energy Conference (EWTEC 2015)*, Pap. 09D2-5. Southampton, UK: Tech. Comm. Eur. Wave Tidal Energy Conf.

Corke TC, Thomas FO. 2015. Dynamic stall in pitching airfoils: aerodynamic damping and compressibility effects. *Annu. Rev. Fluid Mech.* 47:479–505

Creed MJ, Draper S, Nishino T, Borthwick AGL. 2017. Flow through a very porous obstacle in a shallow channel. *Proc. R. Soc. A* 473(2200):20160672

Culley DM, Funke SW, Kramer SC, Piggott MD. 2016. Integration of cost modelling within the micro-siting design optimisation of tidal turbine arrays. *Renew. Energy* 85:215–27

Cummins PF. 2013. The extractable power from a split tidal channel: an equivalent circuit analysis. *Renew. Energy* 50:395–401

De Dominicis M, O'Hara Murray R, Wolf J. 2017. Multi-scale ocean response to a large tidal stream turbine array. *Renew. Energy* 114:1160–79

Divett T, Vennell R, Stevens C. 2013. Optimization of multiple turbine arrays in a channel with tidally reversing flow by numerical modelling with adaptive mesh. *Philos. Trans. R. Soc. A* 371(1985):20120251

Draper S, Adcock TAA, Borthwick AGL, Houlsby GT. 2014. An electrical analogy for the Pentland Firth tidal stream power resource. *Proc. R. Soc. A* 470(2161):20130207

Draper S, Houlsby GT, Oldfield MLG, Borthwick AGL. 2010. Modelling tidal energy extraction in a depth-averaged coastal domain. *IET Renew. Power Gen.* 4(6):545–54

Draper S, Nishino T. 2014. Centred and staggered arrangements of tidal turbines. *J. Fluid Mech.* 739:72–93

Draper S, Stallard T, Stansby P, Way S, Adcock T. 2013. Laboratory scale experiments and preliminary modelling to investigate basin scale tidal stream energy extraction. In *Proceedings of the 10th European Wave and Tidal Energy Conference (EWTEC 2013)*, ed. P Frigaard, JP Kofoed, AS Bahaj, L Bergdahl, A Clément, et al., Pap. 890. Southampton, UK: Tech. Comm. Eur. Wave Tidal Energy Conf.

EMEC (Eur. Mar. Energy Cent.). 2009. *Assessment of tidal energy resource*. Tech. Pap., Eur. Mar. Energy Cent., Stromness, UK

Funke SW, Farrell PE, Piggott MD. 2014. Tidal turbine array optimisation using the adjoint approach. *Renew. Energy* 63:658–73

Garrett C, Cummins P. 2005. The power potential of tidal currents in channels. *Proc. R. Soc. A* 461(2060):2563–72

Garrett C, Cummins P. 2007. The efficiency of a turbine in a tidal channel. *J. Fluid Mech.* 588:243–51

Garrett C, Cummins P. 2008. Limits to tidal current power. *Renew. Energy* 33(11):2485–90

Garrett C, Cummins P. 2013. Maximum power from a turbine farm in shallow water. *J. Fluid Mech.* 714:634–43

Garrett C, Greenberg D. 1977. Predicting changes in tidal regime: the open boundary problem. *J. Phys. Oceanogr.* 7(2):171–81

Glauert H. 1935. *Aerodynamic Theory*. Berlin: Springer

Godin G. 1970. The resolution of tidal constituents. *Int. Hydrogr. Rev.* 47(2):133–44

Greaves D, Iglesias G. 2018. *Wave and Tidal Energy*. Chichester, UK: Wiley

Greenwood C, Vogler A, Venugopal V. 2019. On the variation of turbulence in a high-velocity tidal channel. *Energies* 12(4):672

Grogan DM, Leen SB, Kennedy CR, Ó Brádaigh CM. 2013. Design of composite tidal turbine blades. *Renew. Energy* 57:151–62

Hansen MOL, Johansen J. 2004. Tip studies using CFD and comparison with tip loss models. *Wind Energy* 7:343–56

Hendershott M, Munk W. 1970. Tides. *Annu. Rev. Fluid Mech.* 2(1):205–24

Horwitz RM, Hay AE. 2017. Turbulence dissipation rates from horizontal profiles at mid-depth in fast tidal flows. *Renew. Energy* 114:283–96

Hunter W, Nishino T, Willden RHJ. 2015. Investigation of tidal turbine array tuning using 3D Reynolds-averaged Navier–Stokes simulations. *Int. J. Mar. Energy* 10:39–51

Karsten RH, McMillan JM, Lickley MJ, Haynes RD. 2008. Assessment of tidal current energy in the Minas Passage, Bay of Fundy. *Proc. Inst. Mech. Eng.* 222(5):493–507

Lewis M, McNaughton J, Márquez-Dominguez C, Todeschini G, Togneri M, et al. 2019. Power variability of tidal-stream energy and implications for electricity supply. *Energy* 183:1061–74

McNaughton J, Cao B, Vogel CR, Willden RHJ. 2019. Model scale testing of multi-rotor arrays designed to exploit constructive interference effects. In *Proceedings of the 13th European Wave and Tidal Energy Conference (EWTEC 2019)*, Pap. 1338. Southampton, UK: Tech. Comm. Eur. Wave Tidal Energy Conf.

Milne IA, Day AH, Sharma RN, Flay RGJ. 2015. Blade loading on tidal turbines for uniform unsteady flow. *Renew. Energy* 77:338–50

Milne IA, Day AH, Sharma RN, Flay RGJ. 2016. The characterisation of the hydrodynamic loads on tidal turbines due to turbulence. *Renew. Sustain. Energy Rev.* 56:851–64

Mycek P, Benoît G, Germain G, Pinon G, Rivoalen E. 2014a. Experimental study of the tubulence intensity effects on marine current turbines behaviour. Part I: one single turbine. *Renew. Energy* 66:729–46

Mycek P, Gaurier B, Germain G, Pinon G, Rivoalen E. 2014b. Experimental study of the tubulence intensity effects on marine current turbines behaviour. Part II: two interacting turbines. *Renew. Energy* 68:876–92

Neill SP, Angeloudis A, Robins PE, Walkington I, Ward SL, et al. 2018. Tidal range energy resource and optimization—past perspectives and future challenges. *Renew. Energy* 127:763–78

Neill SP, Hashemi MR. 2018. *Fundamentals of Ocean Renewable Energy: Generating Electricity from the Sea*. London: Academic

Neill SP, Hashemi MR, Lewis MJ. 2016. Tidal energy leasing and tidal phasing. *Renew. Energy* 85:580–87

Ning A, Dykes K. 2014. Understanding the benefits and limitations of increasing maximum rotor tip speed for utility scale wind turbines. *J. Phys. Conf. Ser.* 524:012087

Nishino T, Willden RHJ. 2012. The efficiency of an array of tidal turbines partially blocking a wide channel. *J. Fluid Mech.* 708:596–606

Nishino T, Willden RHJ. 2013. Two-scale dynamics of flow past a partial cross-stream array of tidal turbines. *J. Fluid Mech.* 730:220–44

Norris JV, Droniou E. 2007. Update on EMEC activities, resource description, and characterisation of wave-induced velocities in a tidal flow. In *Proceedings of the 7th European Wave and Tidal Energy Conference (EWTEC 2007)*. Southampton, UK: Tech. Comm. Eur. Wave Tidal Energy Conf.

O'Hara Murray R, Gallego A. 2017. A modelling study of the tidal stream resource of the Pentland Firth, Scotland. *Renew. Energy* 102:326–40

Perez-Campos E, Nishino T. 2015. Numerical validation of the two-scale actuator disc theory for marine turbine arrays. In *Proceedings of the 11th European Wave and Tidal Energy Conference (EWTEC 2015)*, Pap. 09D2-3. Southampton, UK: Tech. Comm. Eur. Wave Tidal Energy Conf.

Polagye BL, Epler J, Thomson J. 2010. Limits to the predictability of tidal current energy. In *Proceedings of the 2010 Oceans Conference*. New York: IEEE

Pugh DT. 1987. *Tides, Surges and Mean Sea-Level*. Chichester, UK: Wiley

Rainey RCT. 2009. The optimum position for a tidal power barrage in the Severn estuary. *J. Fluid Mech.* 636:497–507

Ren Y, Liu B, Zhang T, Fang Q. 2017. Design and hydrodynamic analysis of horizontal axis tidal stream turbines with winglets. *Ocean Eng*. 144:374–83

Ross H, Polagye B. 2020. An experimental assessment of analytical blockage corrections for turbines. *Renew. Energy* 152:1328–41

Rourke FO, Boyle F, Reynolds A. 2010. Tidal energy update 2009. *Appl. Energy* 87(2):398–409

Scarlett GT, Sellar B, van den Bremer T, Viola IM. 2019. Unsteady hydrodynamics of a full-scale tidal turbine operating in large wave conditions. *Renew. Energy* 143:199–213

Schluntz J, Willden RHJ. 2015. The effect of blockage on tidal turbine rotor design and performance. *Renew. Energy* 81:432–41

Sequeira CL, Miller RJ. 2014. Unsteady gust response of tidal stream turbines. In *Proceedings of the 2014 Oceans Conference*. New York: IEEE

Shen WZ, Mikkelsen R, Sørenson JN, Bak C. 2005. Tip loss corrections for wind turbine computations. *Wind Energy* 8:457–75

Shives M, Crawford C. 2016. Adapted two-equation turbulence closures for actuator disk RANS simulations of wind & tidal turbine wakes. *Renew. Energy* 92:279–92

Sørensen JN. 2011. Aerodynamic aspects of wind energy conversion. *Annu. Rev. Fluid Mech.* 43:427–48

Stallard T, Feng T, Stansby PK. 2015. Experimental study of the mean wake of a tidal stream rotor in a shallow turbulent flow. *J. Fluids Struct.* 54:235–46

Stansby PK. 2006. Limitations of depth-averaged modeling for shallow wakes. *J. Hydraul. Eng.* 132(7):737–40

Stansby P, Stallard T. 2016. Fast optimisation of tidal stream turbine positions for power generation in small arrays with low blockage based on superposition of self-similar far-wake velocity deficit profiles. *Renew. Energy* 92:366–75

Stevens RJAM, Meneveau C. 2017. Flow structure and turbulence in wind farms. *Annu. Rev. Fluid Mech.* 49:311–39

Stock-Williams C, Parkinson S, Gunn K. 2013. An investigation of uncertainty in yield prediction for tidal current farms. In *Proceedings of the 10th European Wave and Tidal Energy Conference (EWTEC 2013)*, ed. P Frigaard, JP Kofoed, AS Bahaj, L Bergdahl, A Clément, et al., Pap. 794. Southampton, UK: Tech. Comm. Eur. Wave Tidal Energy Conf.

Thiébot J, Guillou N, Guillou S, Good A, Lewis M. 2020a. Wake field study of tidal turbines under realistic flow conditions. *Renew. Energy* 151:1196–208

Thiébot J, Guillou S, Droniou E. 2020b. Influence of the 18.6-year lunar nodal cycle on the tidal resource of the Alderney Race, France. *Appl. Ocean Res.* 97:102107

Thomson J, Polagye B, Durgesh V, Richmond MC. 2012. Measurements of turbulence at two tidal energy sites in Puget Sound, WA. *IEEE J. Ocean. Eng.* 37(3):363–74

van Kuik GAM. 2007. The Lanchester–Betz–Joukowsky limit. *Wind Energy* 10(3):289–91

Vennell R. 2010. Tuning turbines in a tidal channel. *J. Fluid Mech.* 663:253–67

Vennell R. 2013. Exceeding the Betz limit with tidal turbines. *Renew. Energy* 55:277–85

Vennell R. 2016. An optimal tuning strategy for tidal turbines. *Proc. R. Soc. A* 472(2195):20160047

Vennell R, Adcock TAA. 2014. Energy storage inherent in large tidal turbine farms. *Proc. R. Soc. A* 470(2166):20130580

Vennell R, Funke SW, Draper S, Stevens C, Divett T. 2015. Designing large arrays of tidal turbines: a synthesis and review. *Renew. Sustain. Energy Rev.* 41:454–72

Vogel CR, Houlsby GT, Willden RHJ. 2016. Effect of free surface deformation on the extractable power of a finite width turbine array. *Renew. Energy* 88:317–24

Vogel CR, Willden RHJ. 2017. Multi-rotor tidal stream turbine fence performance and operation. *Int. J. Mar. Energy* 19:198–206

Vogel CR, Willden RHJ. 2018. Designing multi-rotor tidal turbine fences. *Int. J. Mar. Energy* 1(1):61–70

Vogel CR, Willden RHJ, Houlsby GT. 2017. Power available from a depth-averaged simulation of a tidal turbine array. *Renew. Energy* 114:513–24

Vogel CR, Willden RHJ, Houlsby GT. 2018. Blade element momentum theory for a tidal turbine. *Ocean Eng.* 169:215–26

Vogel CR, Willden RHJ, Houlsby GT. 2019. Tidal stream turbine power capping in a head-driven tidal channel. *Renew. Energy* 136:491–99

Wang T, Adcock TAA. 2019. Combined power and thrust capping in the design of tidal turbine farms. *Renew. Energy* 133:1247–56

Whelan JI, Graham JMR, Peiró J. 2009. Inertia effects on horizontal axis tidal stream turbines. In *Proceedings of the 8th European Wave and Tidal Energy Conference (EWTEC 2009)*, Pap. 225. Southampton, UK: Tech. Comm. Eur. Wave Tidal Energy Conf.

Wimshurst A, Vogel CR, Willden RHJ. 2018. Cavitation limits on tidal turbine performance. *Ocean Eng.* 152:223–33

Wimshurst A, Willden RHJ. 2017. Analysis of a tip correction factor for horizontal axis turbines. *Wind Energy* 20:1515–28

Wimshurst A, Willden RHJ. 2018. Computational observations of the tip loss mechanism experienced by horizontal axis rotors. *Wind Energy* 21:544–57

Young AM, Smyth ASM, Bajpai V, Augarde RF, Farman JR, Sequeira CL. 2019. Improving tidal turbine efficiency using winglets. In *Proceedings of the 13th European Wave and Tidal Energy Conference (EWTEC 2019)*, Pap. 1635. Southampton, UK: Tech. Comm. Eur. Wave Tidal Energy Conf.

Zhang L, Wang S, Sheng Q, Jing F, Ma Y. 2015. The effects of surge motion of the floating platform on hydrodynamics performance of horizontal axis tidal current turbine. *Renew. Energy* 74:796–802

Zilic de Arcos F, Vogel CR, Willden RHJ. 2019. Hydrodynamic modelling of flexible tidal turbine blades. In *Proceedings of the 13th European Wave and Tidal Energy Conference (EWTEC 2019)*, Pap. 1587. Southampton, UK: Tech. Comm. Eur. Wave Tidal Energy Conf.